

# Nonadiabatic Tunneling in Photodissociation of Phenol

Changjian Xie,<sup>†,||</sup> Jianyi Ma,<sup>§</sup> Xiaolei Zhu,<sup>#</sup> David R. Yarkony,<sup>\*,#</sup> Daiqian Xie,<sup>\*,||,⊥</sup> and Hua Guo<sup>\*,†</sup>

<sup>†</sup>Department of Chemistry and Chemical Biology, University of New Mexico, Albuquerque, New Mexico 87131, United States

<sup>||</sup>Institute of Theoretical and Computational Chemistry, Key Laboratory of Mesoscopic Chemistry, School of Chemistry and Chemical Engineering, Nanjing University, Nanjing 210093, China

<sup>§</sup>Institute of Atomic and Molecular Physics, Sichuan University, Chengdu, Sichuan 610065, China

<sup>#</sup>Department of Chemistry, Johns Hopkins University, Baltimore, Maryland 21218, United States

<sup>⊥</sup>Synergetic Innovation Center of Quantum Information and Quantum Physics, University of Science and Technology of China, Hefei, Anhui 230026, China

## Supporting Information

**ABSTRACT:** Using recently developed full-dimensional coupled quasi-diabatic *ab initio* potential energy surfaces including four electronic ( $^1\pi\pi$ ,  $^1\pi\pi^*$ ,  $^1\pi\sigma^*$ , and  $2^1\pi\sigma^*$ ) states, the tunneling dynamics of phenol photodissociation via its first excited singlet state ( $S_1 \leftarrow S_0$ ) is investigated quantum mechanically using a three-dimensional model. The lifetimes of several low-lying vibrational states are examined and compared with experiment. The deuteration of the phenoxy hydrogen is found to dramatically increase the lifetime, attesting to the tunneling nature of the nonadiabatic dissociation. Importantly, it is shown that owing to the conical intersection topography tunneling in this system cannot be described in the standard adiabatic approximation, which eschews the geometric phase effect since the nonadiabatically computed lifetimes, validated by comparison with experiment, differ significantly from those obtained in that limit.

The breakdown of the Born–Oppenheimer (BO) approximation is prevalent in photochemistry because of the increased probabilities of degeneracies among excited electronic states.<sup>1</sup> These nonadiabatic processes are important for understanding a wide array of phenomena, including photoisomerization,<sup>2</sup> internal conversion,<sup>3</sup> and photovoltaics.<sup>4</sup> Despite much effort, our understanding of the dynamics of non-BO processes is still far from complete.<sup>5</sup> This has in part motivated the study of nonadiabatic photodissociation dynamics of small molecules such as water and ammonia, which are strongly affected by conical intersections (CIs).<sup>6</sup> We have recently demonstrated that a complete understanding of such systems can be achieved, with the help of accurate coupled potential energy surfaces (PESs)<sup>7,8</sup> and nonadiabatic quantum dynamics.<sup>9–14</sup>

In larger systems, the increased number of degrees of freedom (DOFs) complicates the nonadiabatic dynamics. It is essential to extend our theoretical models to such systems in order to understand the impact of this increasing complexity. The dissociation of phenol ( $C_6H_5OH$ ) with 33 internal DOFs is a particularly intriguing problem with implications for photochemistry of cyclic moieties in amino acids.<sup>3,15,16</sup> Consequently it has been the subject of experimental studies

by several groups using state-of-the-art techniques.<sup>17–30</sup> Dissociation on the  $S_1$  state, initiated by an excitation based on the phenoxy ring, produces an H atom and a phenoxy radical ( $C_6H_5O$ ).<sup>20,21</sup> The fragment kinetic energy distribution is structured and wavelength dependent, providing valuable information concerning the internal energy distribution of the phenoxy product,<sup>20–22,25–27,30</sup> which in turn reflects nonadiabatic dissociation dynamics. At low energies, experimental evidence, including real time measurements<sup>29</sup> and isotope effects,<sup>18</sup> strongly suggest that the dissociation is via tunneling.

The nonadiabatic dissociation pathways of phenol were first mapped out by Sobolewski and Domcke,<sup>31</sup> using theoretical method. This pioneering work revealed that dissociation from the first excited state,  $S_1$  with  $^1\pi\pi^*$  character involves two seams of CIs as a largely repulsive state with  $^1\pi\sigma^*$  character intersects both the  $S_0$  and  $S_1$  states. The dissociation of low-lying vibrational levels of the  $S_1$  state, which can only be initiated by tunneling, proceeds nonadiabatically via the CI coupling of the  $S_1$  and  $S_2$  states; see Figure 1. Quantum dissociation dynamics was investigated using two-dimensional models on coupled PESs based on *ab initio* data.<sup>23,32–34</sup> Deuteration was found to slow the dissociation.<sup>35</sup> Recently, there have been efforts to map out higher-,<sup>36</sup> and full-dimensional quasi-diabatic PESs for this system.<sup>37–40</sup> Truhlar and co-workers (YXZT) have reported<sup>39</sup> three full-dimensional coupled PESs, fit to a large number of points determined from multiconfiguration quasi-degenerate perturbation theory using their anchor-points reactive potential method.<sup>41</sup> Zhu and Yarkony (ZY) have also reported full-dimensional coupled PESs based on multi-reference configuration interaction single and double excitation expansions.<sup>40</sup> In the latest version, energies, gradients, and derivative couplings at 7379 geometries were fit.<sup>42</sup> Nonadiabatic dynamics on these multidimensional PESs has been explored using semiclassical methods, with<sup>43</sup> and without tunneling.<sup>40</sup>

It is important to point out that atomic tunneling in molecular systems is often treated within the BO approximation, characterized by a barrier on an adiabatic PES.<sup>44</sup> The nonadiabatic nature of phenol photodissociation presents a

Received: April 4, 2016

Published: June 9, 2016

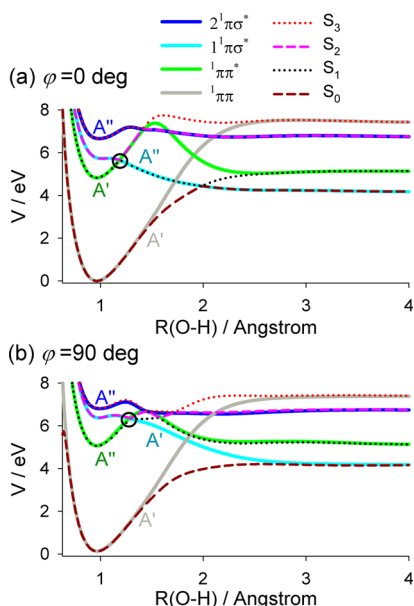


**Figure 1.** Adiabatic (dashed lines) and diabatic (solid lines) potential energy curves of the sZY PESs as a function of  $R(\text{O-H})$  at  $\varphi = 0$  and  $90^\circ$ , respectively. Other coordinates are fixed at the  $S_0$  equilibrium. The ordering/labeling of the diabats is appropriate to the Franck-Condon region. The  $S_1$ - $S_2$  CI is circled.

unique opportunity for studying the dynamics of nonadiabatic tunneling,<sup>45</sup> namely, tunneling beyond the BO limit.<sup>23,34,46,47</sup> To this end, it is imperative to treat the dynamics quantum mechanically because neither tunneling nor nonadiabaticity has a classical analog. Indeed, as we demonstrate below, the adiabatic treatment provides a very poor description of tunneling in phenol. The utility of the adiabatic approximation has been considered from an alternative perspective in ref 43.

The recently developed full-dimensional coupled PESs for phenol offer accurate and efficient platforms to carry out quantum dynamical studies of the nonadiabatic dissociation. As a first effort in this direction, we report here a reduced-dimensional model for the nonadiabatic dissociation dynamics of phenol initially excited to the  $S_1$  state, using the Zhu-Yarkony coupled PESs. The dynamics of both phenol ( $\text{C}_6\text{H}_5\text{OH}$ ) and its deuterated isotopomer ( $\text{C}_6\text{H}_5\text{OD}$ ) are described by quantum wave packets. A key question to be addressed is how nonadiabaticity affects the tunneling dynamics.

Figure 2 depicts the OH stretch, COH bend, and CCOH torsion, ( $R, \theta, \varphi$ ), in our three-dimensional (3D) model. They

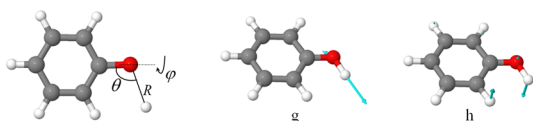


**Figure 2.** Left panel: coordinates ( $R, \theta, \varphi$ ) used in the 3D calculations. Right panel: the  $g$  and  $h$  vectors at the  $S_1$ - $S_2$  MEX.

are the disappearing coordinates in the photodissociation, thus are necessarily involved in the dynamics.<sup>36</sup> This choice is also supported by the analysis of the  $g$  and  $h$  vectors, the energy difference gradient and coupling gradient vectors,<sup>6</sup> for the CI connecting  $S_1$  and  $S_2$  states. These two vectors define a unique plane, the branching plane of the CI, which allows for the

conceptual separation of the conical intersection coordinates from the remaining nuclear DOFs, regardless of the size of the molecule, and play a crucial role in both describing and computing nonadiabatic transitions near CIs.<sup>32,33,36,40</sup> When phenol normal vibrational mode vectors, shown in Figure 2, are projected onto the mass scaled  $g$  and  $h$  vectors at the minimum energy crossing point (MEX) of this CI, the largest overlaps (0.927 with  $g$  and 0.934 with  $h$ ) are the O-H vibrational and the C-C-O-H torsional coordinates, respectively. Our analysis thus supports the argument of Lan et al.<sup>32</sup> that these two coordinates are the main participants of the nonadiabatic tunneling involving the  $S_1$ - $S_2$  CI. The complete table of the overlaps can be found in the Supporting Information (SI).

The nuclear Hamiltonian of the multistate system defined in the diabatic representation is given as follows:<sup>40</sup>

$$\mathbf{H}^d = \hat{T} \begin{pmatrix} 1 & 0 & 0 & 0 \\ 0 & 1 & 0 & 0 \\ 0 & 0 & 1 & 0 \\ 0 & 0 & 0 & 1 \end{pmatrix} + \begin{pmatrix} V_{11} & V_{12} & V_{13} & V_{14} \\ V_{21} & V_{22} & V_{23} & V_{24} \\ V_{31} & V_{32} & V_{33} & V_{34} \\ V_{41} & V_{42} & V_{43} & V_{44} \end{pmatrix} \quad (1)$$

where  $\hat{T}$  is the kinetic energy operator and  $V_{11}, V_{22}, V_{33}$ , and  $V_{44}$  are the potential energies of the  ${}^1\pi\pi$ ,  ${}^1\pi\pi^*$ ,  ${}^1\pi\sigma^*$ , and  ${}^2\pi\sigma^*$  quasi diabatic states, respectively, with the off-diagonal elements as the couplings. The diagonalization of  $\mathbf{V}$  yields the  $S_0, S_1, S_2$ , and  $S_3$  adiabatic states. The version of the ZY PESs used here has been adjusted by shifting the  ${}^1\pi\pi^*$  and  ${}^1\pi\sigma^*$  diabatic states down by 0.2232 and 0.1288 eV, respectively, in order to achieve better agreement with experimental energetics.<sup>42</sup> Figure 1a,b shows the adiabatic and diabatic potential curves ( $\varphi = 0$  and  $90^\circ$ ) of the shifted ZY (denoted as sZY) PESs as a function of O-H bond distance with other coordinates fixed at the equilibrium geometry of the  $S_0$  state. The details of the diabatic PESs can be found in recent publications by two of the current authors.<sup>40,42</sup> Other details of the Hamiltonian are given in SI.

In this work, we focus on the photodissociation dynamics of phenol in its first singlet excited ( $S_1$ ) state. The lowest few vibrational levels (listed in SI) are above the dissociation asymptote, but significantly below both the  $S_1$  dissociation saddle point and the MEX for the  $S_1$ - $S_2$  CI, which are, respectively, 5152 and 6593  $\text{cm}^{-1}$  above the  $S_1$  minimum with a planar ( $\varphi = 0$ ) geometry. Hence, these levels are predissociative, facilitated by tunneling via the CI or through the  $S_1$  saddle point. It is difficult to accurately characterize the multidimensional tunneling dynamics without quantum mechanics. Even with the 3D model, a brute-force approach is impractical because the propagation required is too long for these long-lived ( $\sim$ ns) resonances. A low-storage filter diagonalization method<sup>48</sup> was used to determine their lifetimes,  $\tau = 1/\Gamma$ , in which a wave packet is propagated using the Chebyshev propagator, and the resulting correlation functions are used to build an energy-localized Hamiltonian matrix, from which the complex energies of the resonances ( $E - i\Gamma/2$ ) are obtained.<sup>49,50</sup>

Table 1 reports the lifetimes of several low-lying vibrational states for  $\text{C}_6\text{H}_5\text{OH}$  and  $\text{C}_6\text{H}_5\text{OD}$ , in which  $\nu = 1, 2, 3$  stand for the  $\nu_{\text{OH}}$ ,  $\beta_{\text{COH}}$ , and  $\tau_{\text{OH}}$  modes in the Wilson notation, respectively. Clearly, the lifetimes are mode specific and isotope dependent. This is consistent with previous quantum dynamical calculations in lower dimensions.<sup>23,32-35</sup> Unfortunately, none of the earlier quantum studies reported lifetimes, due apparently to the difficulties alluded to above.

**Table 1.** Calculated Lifetimes of Low-Lying Vibrational Levels on the  $S_1$  State

| $\nu^n$ | lifetime (ns) |            |
|---------|---------------|------------|
|         | $C_6H_5OH$    | $C_6H_5OD$ |
| $0^0$   | 2.29          | 770        |
| $3^1$   | 0.71          | 240        |
| $2^1$   | 0.69          | 160        |
| $1^1$   | 0.00049       | 0.046      |

For the lowest vibrational level ( $0^0$ ) of phenol on the  $S_1$  state, our calculated lifetime of 2.29 ns is in reasonably good agreement with the experimental values of  $2.4 \pm 0.3$ ,<sup>18</sup>  $2.2 \pm 0.1$ ,<sup>28</sup> and  $>1.2$  ns.<sup>29</sup> The much longer lifetime for  $C_6H_5OD$  is consistent with the absence of an experimentally measurable D signal.<sup>21</sup> It is also consistent with theoretical estimates of a  $10^3$  reduction of the tunneling probability upon deuteration.<sup>34</sup> Although the  $S_1$  lifetime of  $C_6H_5OD$  and  $C_6D_5OD$  has been measured (16.2<sup>51</sup> and 13.3 ns<sup>18</sup>), it reflects mostly the radiative decay, which is expected to be more facile than the tunneling facilitated dissociation. This level of agreement with the experimental tunneling lifetimes indicates that the tunneling dynamics is reasonably well described by the 3D model.

To illustrate the tunneling dynamics, the time-independent diabatic wave functions of the  $1^1\pi\pi^*$  and  $1^1\pi\sigma^*$  states corresponding to the  $0^0$  resonance of  $C_6H_5OH$  is shown in Figure 3 in which  $\theta$  is fixed at  $109.5^\circ$ . It is shown that the wave

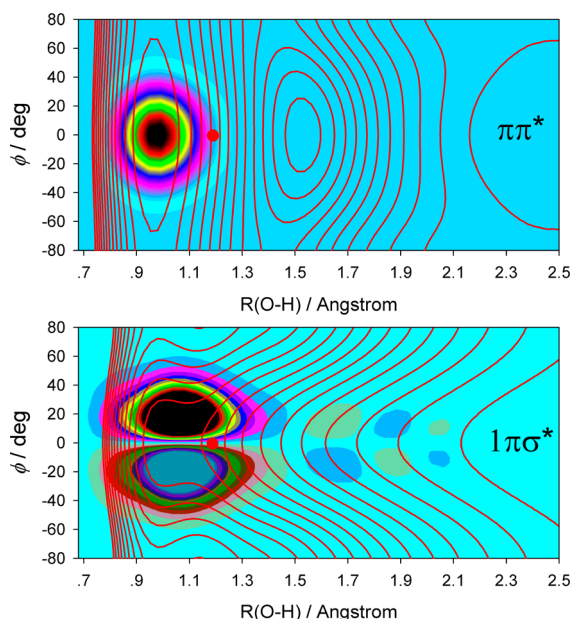


**Figure 3.** Diabatic wave functions of the  $1^1\pi\pi^*$  and  $1^1\pi\sigma^*$  states corresponding to the  $0^0$  resonance, with the C–O–H bending angle fixed at  $109.5^\circ$ . The diabatic potential contours are superimposed on the wave functions and the  $S_1$ – $S_2$  MEX is marked as a red dot.

functions are mostly near the planar ( $\varphi = 0$ ) region in the vicinity of the  $S_1$ – $S_2$  MEX (marked in the figure by a red dot). Furthermore, it is clear from the figure that the two diabatic wave functions are qualitatively different. The preeminent contributor (99.8% of the norm) on the  $1^1\pi\pi^*$  diabat is nodeless in  $\varphi$ , while that on the  $1^1\pi\sigma^*$  diabat has a node at  $\varphi = 0$ . The difference stems from the fact that the total vibronic symmetry of the  $1^1\pi\pi^*$  and  $1^1\pi\sigma^*$  diabats, which have  $A'$  and  $A''$  electronic

symmetry in planar geometries, respectively, must be the same. The nonadiabatic transition through the CI necessitates a switch of the vibrational character. Since the total (electronic and nuclear) wave function has to be symmetric, the nuclear wave function on the  $1^1\pi\sigma^*$  state has to be antisymmetric.<sup>23,34,46,47</sup> Indeed, the off-diagonal element ( $V_{23}$ ) between the two diabatic states, which facilitates the transition, has antisymmetric reflection symmetry with respect to  $\varphi = 0$ .

We have also computed the tunneling lifetimes using a fully quantum mechanical adiabatic model in which only the  $S_1$  adiabat was used in solving the Schrödinger equation. For the  $0^0$  resonance of phenol, the adiabatic tunneling lifetime is calculated to be 0.027 ns, about 100 times shorter than the correct value. This large difference demonstrates that the adiabatic model is not appropriate for the description of tunneling near a CI. One possible reason is the geometric phase (GP) effect, which introduces a phase factor ( $-1$ ) for the adiabatic electronic wave function transported along a closed loop around a CI,<sup>52–54</sup> and is ignored in standard adiabatic state calculations. Mead and Truhlar pointed out the importance of the GP effect when, from a quantum mechanical perspective, interference between “trajectories” passing on opposite sides of a CI is possible.<sup>52</sup> While the size of the GP effect can only be determined by including the GP in actual calculations, ample examples have demonstrated that the GP needs to be considered in treating adiabatic dynamics around a CI.<sup>55–58</sup> Our results here are reminiscent of the recent observation of spatial localization near a CI, which can only be reproduced in the adiabatic representation with the proper inclusion of the GP.<sup>59</sup> Quantification of the GP effect requires its explicit inclusion in the single state adiabatic model. In the diabatic representation, the GP effect is automatically included, but so are both electronic states.

In this work, we reported a 3D wave packet study of the photodissociation dynamics of phenol in the  $S_1$  state based on newly constructed full-dimensional coupled diabatic PESs. Our results confirm the tunneling nature of the dissociation and report for the first time quantum mechanical tunneling lifetimes. The computed lifetime of  $C_6H_5OH$  in its  $0^0$  level of 2.29 ns is in excellent agreement with available experimental data. A huge isotope effect was found for the dissociation lifetime of  $C_6H_5OD$ , which is also consistent with known observations. The agreement with available experimental data on tunneling suggests that the reduced-dimensional model is sufficient to describe the initial stage of the nonadiabatic dissociation of phenol.

Perhaps more importantly, our calculations demonstrate that for the encountered topography of a low energy conical intersection nonadiabatic tunneling dynamics cannot be correctly characterized with the standard adiabatic state model. Inclusion of the GP effect is expected to reduce the discrepancy. However, more detailed studies including the GP are needed and planned to quantify the size of the effect. Future studies will also be higher dimensional to understand the role of other vibrational modes in phenol photodissociation.

## ■ ASSOCIATED CONTENT

### 📄 Supporting Information

The Supporting Information is available free of charge on the ACS Publications website at DOI: 10.1021/jacs.6b03288.

Details of the model and calculations as well as additional results (PDF)



## ■ AUTHOR INFORMATION

## Corresponding Authors

\*yarkony@jhu.edu

\*dqxie@nju.edu.cn

\*hguo@unm.edu

## Notes

The authors declare no competing financial interest.

## ■ ACKNOWLEDGMENTS

We thank US Department of Energy (DE-FG02-05ER15694 to H.G. and DE-FG02-91ER14189 to D.R.Y.) and by National Natural Science Foundation of China (21403104, 21133006, 21590802, 91421315 to D.X. and 91441107 to J.M.) and the Chinese Ministry of Science and Technology (2013CB834601 to D.X.). This research used resources of the National Energy Research Scientific Computing Center, a DOE Office of Science User Facility supported by the Office of Science of the U.S. Department of Energy under Contract No. DE-AC02-05CH11231. The coupled potential energy surfaces used in this work and the programs that generated them are available on the open source site GITHUB as follows: coupled potential surfaces, <https://github.com/virtualzx-nad/phenol-Hd>; fitting program and surface evaluation library, <https://github.com/virtualzx-nad/surfgen>.

## ■ REFERENCES

- (1) Klessinger, M.; Michl, J. *Excited States and Photochemistry of Organic Molecules*; VCH: New York, 1995.
- (2) Levine, B. G.; Martínez, T. J. *Annu. Rev. Phys. Chem.* **2007**, *58*, 613.
- (3) Matsika, S.; Krause, P. *Annu. Rev. Phys. Chem.* **2011**, *62*, 621.
- (4) Zhugayevych, A.; Tretiak, S. *Annu. Rev. Phys. Chem.* **2015**, *66*, 305.
- (5) Tully, J. C. *J. Chem. Phys.* **2012**, *137*, 22A301.
- (6) Yarkony, D. R. *Chem. Rev.* **2012**, *112*, 481.
- (7) Jiang, B.; Xie, D.; Guo, H. *J. Chem. Phys.* **2012**, *136*, 034302.
- (8) Zhu, X.; Ma, J.; Yarkony, D. R.; Guo, H. *J. Chem. Phys.* **2012**, *136*, 234301.
- (9) Zhou, L.; Jiang, B.; Xie, D.; Guo, H. *J. Phys. Chem. A* **2013**, *117*, 6940.
- (10) Zhou, L.; Xie, D.; Guo, H. *J. Chem. Phys.* **2015**, *142*, 124317.
- (11) Ma, J.; Zhu, X.; Guo, H.; Yarkony, D. R. *J. Chem. Phys.* **2012**, *137*, 22A541.
- (12) Ma, J.; Xie, C.; Zhu, X.; Yarkony, D. R.; Xie, D.; Guo, H. *J. Phys. Chem. A* **2014**, *118*, 11926.
- (13) Xie, C.; Ma, J.; Zhu, X.; Zhang, D. H.; Yarkony, D. R.; Xie, D.; Guo, H. *J. Phys. Chem. Lett.* **2014**, *5*, 1055.
- (14) Xie, C.; Zhu, X.; Ma, J.; Yarkony, D. R.; Xie, D.; Guo, H. *J. Chem. Phys.* **2015**, *142*, 091101.
- (15) Sobolewski, A. L.; Domcke, W.; Dedonder-Lardeux, C.; Jouvet, C. *Phys. Chem. Chem. Phys.* **2002**, *4*, 1093.
- (16) Ashfold, M. N. R.; King, G. A.; Murdock, D.; Nix, M. G. D.; Oliver, T. A. A.; Sage, A. G. *Phys. Chem. Chem. Phys.* **2010**, *12*, 1218.
- (17) Bist, H. D.; Brand, J. C. D.; Williams, D. R. *J. Mol. Spectrosc.* **1966**, *21*, 76.
- (18) Ratzer, C.; Küpper, J.; Spangenberg, D.; Schmitt, M. *Chem. Phys.* **2002**, *283*, 153.
- (19) Tseng, C. M.; Lee, Y. T.; Ni, C. K. *J. Chem. Phys.* **2004**, *121*, 2459.
- (20) Ashfold, M. N. R.; Cronin, B.; Devine, A. L.; Dixon, R. N.; Nix, M. G. D. *Science* **2006**, *312*, 1637.
- (21) Nix, M. G. D.; Devine, A. L.; Cronin, B.; Dixon, R. N.; Ashfold, M. N. R. *J. Chem. Phys.* **2006**, *125*, 133318.
- (22) Tseng, C. M.; Lee, Y. T.; Lin, M. F.; Ni, C. K.; Liu, S. Y.; Lee, Y. P.; Xu, Z. F.; Lin, M. C. *J. Phys. Chem. A* **2007**, *111*, 9463.
- (23) Nix, M. G. D.; Devine, A. L.; Dixon, R. N.; Ashfold, M. N. R. *Chem. Phys. Lett.* **2008**, *463*, 305.
- (24) Ashfold, M. N. R.; Devine, A. L.; Dixon, R. N.; King, G. A.; Nix, M. G. D.; Oliver, T. A. A. *Proc. Natl. Acad. Sci. U. S. A.* **2008**, *105*, 12701.
- (25) Hause, M. L.; Yoon, Y. H.; Case, A. S.; Crim, F. F. *J. Chem. Phys.* **2008**, *128*, 104307.
- (26) Iqbal, A.; Cheung, M. S. Y.; Nix, M. G. D.; Stavros, V. G. *J. Phys. Chem. A* **2009**, *113*, 8157.
- (27) King, G. A.; Oliver, T. A. A.; Nix, M. G. D.; Ashfold, M. N. R. *J. Phys. Chem. A* **2009**, *113*, 7984.
- (28) Pino, G. A.; Oldani, A. N.; Marceca, E.; Fujii, M.; Ishiuchi, S. I.; Miyazaki, M.; Broquier, M.; Dedonder, C.; Jouvet, C. *J. Chem. Phys.* **2010**, *133*, 124313.
- (29) Roberts, G. M.; Chatterley, A. S.; Young, J. D.; Stavros, V. G. *J. Phys. Chem. Lett.* **2012**, *3*, 348.
- (30) Iqbal, A.; Pegg, L. J.; Stavros, V. G. *J. Phys. Chem. A* **2008**, *112*, 9531.
- (31) Sobolewski, A. L.; Domcke, W. *J. Phys. Chem. A* **2001**, *105*, 9275.
- (32) Lan, Z.; Domcke, W.; Vallet, V.; Sobolewski, A. L.; Mahapatra, S. *J. Chem. Phys.* **2005**, *122*, 224315.
- (33) Vieuxmaire, O. P. J.; Lan, Z.; Sobolewski, A. L.; Domcke, W. *J. Chem. Phys.* **2008**, *129*, 224307.
- (34) Dixon, R. N.; Oliver, T. A. A.; Ashfold, M. N. R. *J. Chem. Phys.* **2011**, *134*, 194303.
- (35) An, H.; Baeck, K. K. *J. Phys. Chem. A* **2011**, *115*, 13309.
- (36) Ramesh, S. G.; Domcke, W. *Faraday Discuss.* **2013**, *163*, 73.
- (37) Xu, X.; Yang, K. R.; Truhlar, D. G. *J. Chem. Theory Comput.* **2013**, *9*, 3612.
- (38) Zhu, X.; Yarkony, D. R. *J. Chem. Phys.* **2014**, *140*, 024112.
- (39) Yang, K. R.; Xu, X.; Zheng, J. J.; Truhlar, D. G. *Chem. Sci.* **2014**, *5*, 4661.
- (40) Zhu, X.; Yarkony, D. R. *J. Chem. Phys.* **2016**, *144*, 024105.
- (41) Yang, K. R.; Xu, X.; Truhlar, D. G. *J. Chem. Theory Comput.* **2014**, *10*, 924.
- (42) Zhu, X.; Malbon, C. L.; Yarkony, D. R. *J. Chem. Phys.* **2016**, *144*, 124312.
- (43) Xu, X.; Zheng, J. J.; Yang, K. R.; Truhlar, D. G. *J. Am. Chem. Soc.* **2014**, *136*, 16378.
- (44) Meisner, J.; Kästner, J. *Angew. Chem., Int. Ed.* **2016**, *55*, 2.
- (45) Nakamura, H. *J. Chem. Phys.* **1987**, *87*, 4031.
- (46) Abe, M.; Ohtsuki, Y.; Fujimura, Y.; Lan, Z.; Domcke, W. *J. Chem. Phys.* **2006**, *124*, 224316.
- (47) Bouakline, F. *Chem. Phys.* **2014**, *442*, 31.
- (48) Guo, H. *Rev. Comput. Chem.* **2007**, *25*, 285.
- (49) Mandelshtam, V. A.; Taylor, H. S. *J. Chem. Phys.* **1997**, *106*, 5085.
- (50) Chen, R.; Guo, H. *Chem. Phys. Lett.* **1997**, *279*, 252.
- (51) Lipert, R. J.; Colson, S. D. *J. Phys. Chem.* **1989**, *93*, 135.
- (52) Mead, C. A.; Truhlar, D. G. *J. Chem. Phys.* **1979**, *70*, 2284.
- (53) Berry, M. V. *Proc. R. Soc. London, Ser. A* **1984**, *392*, 45.
- (54) Longuet-Higgins, H. C.; Opik, U.; Pryce, M. H. L.; Sack, R. A. *Proc. R. Soc. London, Ser. A* **1958**, *244*, 1.
- (55) Juanes-Marcos, J. C.; Althorpe, S. C.; Wrede, E. *Science* **2005**, *309*, 1227.
- (56) Jankunas, J.; Sneha, M.; Zare, R. N.; Bouakline, F.; Althorpe, S. C. *J. Chem. Phys.* **2013**, *139*, 144316.
- (57) Kendrick, B. K.; Hazra, J.; Balakrishnan, N. *Nat. Commun.* **2015**, *6*, 7918.
- (58) Kendrick, B. K.; Hazra, J.; Balakrishnan, N. *Phys. Rev. Lett.* **2015**, *115*, 153201.
- (59) Ryabinkin, I. G.; Izmaylov, A. F. *Phys. Rev. Lett.* **2013**, *111*, 220406.